LA-UR- 08-8035

Approved for public release;
distribution is unlimited.

Title:	Local and bulk melting of Cu at grain boundaries
Author(s):	Li-Bo Han, Qi An, Rong-Shan Fu, University of Technology of China Lianqing Zheng, Florida State University Sheng-Nian Luo, LANL
Intended for:	Journal of Chemical Physics

Los Alamos
NATIONAL LABORATORY
EST. 1943

Form 836 (7/06)

Submitted to *Journal of Chemical Physics*

Local and bulk melting of Cu at grain boundaries

Li-Bo Han, Qi An,* and Rong-Shan Fu
School of Earth and Space Sciences, University of Science and Technology of China, Hefei, Anhui, 230026, P.R. China

Lianqing Zheng
Institute of Molecular Biophysics, Florida State University, Tallahassee, FL 32306, USA

Sheng-Nian Luo†
Physics Division, Los Alamos National Laboratory, Los Alamos, NM 87545, USA
(Dated: December 15, 2008)

We investigate gain boundary (GB) melting using molecular dynamics simulations on face-centered-cubic Cu bicrystals with symmetric ⟨110⟩ tilt grain boundaries. The temperature and temporal evolutions of the Cu bicrystals under stepped heating are characterized in terms of order parameters and diffusion coefficients. Premelting of the GB region is negligible within simulation uncertainties, and continuous solid state disordering rather than melting occurs below the thermodynamic melting temperature (T_m). Liquid nuclei form liquid islands within solid matrix in the GB region near T_m. This local melting progresses continuously with time and temperature but is limited by kinetics; consequently, the GB region as a whole is superheated by about $0.13T_m$ before its bulk melting occurs discontinuously.

I. INTRODUCTION

The role of defects in melting has been a subject of extensive theoretical, experimental and modeling investigations.[1–15] Given its high free energy and omnipresence in real solids, grain boundary (GB) is of particular importance in melting, and thus has been investigated in considerable breath and depth.[11–17] Nonetheless, several key issues remain controversial as regards the process and nature of GB melting, including premelting versus superheating, continuous versus discontinuous melting, solid-state disordering versus melting, and local versus bulk melting of the GB region. For instance, both premelting and superheating were claimed by molecular dynamics simulations.[15,17] Limitations in experimental techniques still preclude a conclusion as regards the exact nature of GB melting.[11]

MD simulation is advantageous for its spatial and temporal resolutions unparalleled by experiments. However, comparison among previous MD simulations (as well as experiments) suffers from certain difficulties, e.g., different statistical ensembles are used, the thermodynamic melting temperature (T_m) is not properly calculated, or the definitions of melting are different. In our opinion, melting can be better constrained with diffusion coefficients. The GB region is often assumed to disorder or melt as a whole (bulk melting) and the fine structures (localized melting) within it are neglected. In this study, we use local order parameters and diffusion coefficients to characterize the GB region and its fine structures. We show that solid state disordering rather than premelting occurs below T_m, local melting precedes bulk melting, bulk melting occurs at a considerably superheated state and is first-order in nature, and solid state disordering and local melting are continuous. Sec. II describes the methodology of MD simulations and analyses. The results and discussion are presented in Sec. III, followed by conclusion in Sec. IV.

II. METHODOLOGY

Grain boundaries in face-centered-cubic (fcc) solids have long been studied and we choose a symmetric ⟨110⟩ tilt grain boundary, $\Sigma = 11/(113)/[110]$, since it is a metastable structure in this GB class.[18] Here Σ characterizes the coincident site lattice in a bicrystal, (113) is the GB plane, and the tilt angle is 50.58°. The bicrystals with such GBs are created via the coincidence site lattice constructions.[18] We choose the GB normal as the x-axis. Two system sizes of about 10^5 atoms and 10^6 atoms are explored, and the number of atomic layers along the x-axis is 50 and 100, respectively. Three-dimensional periodic boundary conditions are applied. The interactions among Cu atoms are described by an accurate embedded atom method (EAM) potential.[19] The initial configurations are relaxed with the conjugate gradient technique. We characterize the relaxed configurations with order parameters (see below). The order parameters of the GB region are reduced from 1 to about 0.56–0.9. (The atomic configurations are similar to that at 300 K in Fig. 1.) This disordering and the extra GB energy give rise to heterogeneous nucleation which may completely outrun homogeneous nucleation in MD simulation time scales.

MD simulations are performed on the relaxed bicrystals with the constant-pressure-temerature ensembles

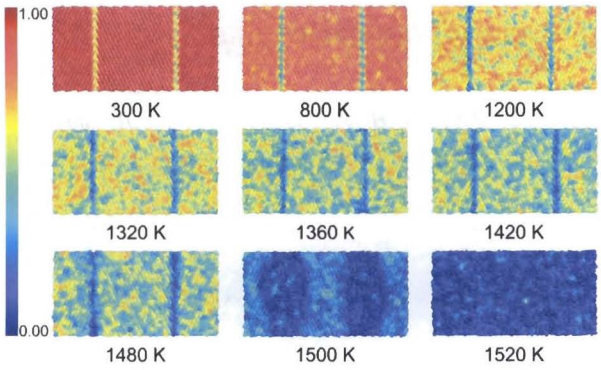

FIG. 1: Atomic configurations of a Cu bicrystal thermalized for 50 ps at representative temperatures, projected along the z-axis. Atoms are color-coded based on local order parameters $\bar{\psi}$.

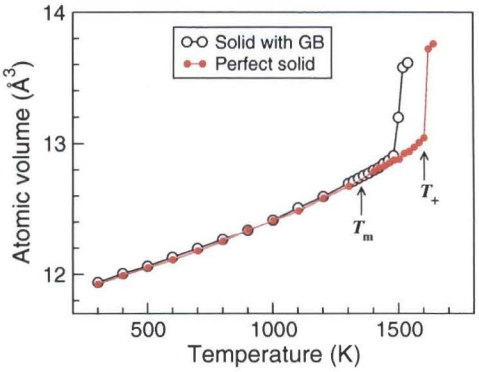

FIG. 2: Atomic volume versus temperature for the Cu bicrystal and a perfect solid during incremental heating. T_m and T_+ denote thermodynamic melting temperature and the maximum superheating temperature, respectively.

and the same EAM potential as for energy minimization. Temperature (T) is controlled with a Hoover thermostat,[20] and the isotropic pressure, with isotropic volume scaling.[21] The solids undergo incremental heating into liquid regime at ambient pressure, and the temperature increment is 20 K at high temperatures for the 10^5 atom system. The time step for integrating the equation of motion is 1 fs. At each temperature, the run duration is 50 ps unless stated otherwise. For the 10^6 atom system, the heating rate is 100 K per 50 ps. For comparison, we also examine the melting of a perfect solid (62 500 atoms) and liquid at similar conditions.

To quantify local and global structure disordering, we calculate the local order parameters of individual atoms and the global order parameter of the whole system.[22] We choose a set of $N_{\mathbf{q}} = 6$ direction vectors $\{\mathbf{q}\}$ satisfying $\exp(i\mathbf{q}\cdot\mathbf{r}) = 1$, for vectors $\{\mathbf{r}\}$ connecting an atom and its neighbors in a perfect fcc solid. For a bicrystal, two sets of $\{\mathbf{q}\}$ are chosen, each for a constituent grain (half the bicrystal). The local order parameter of a specific atom is defined as

$$\psi = \left| \frac{1}{N_{\mathbf{q}}} \frac{1}{N_c} \sum_{\mathbf{r}} \sum_{\mathbf{q}} \exp(i\mathbf{q}\cdot\mathbf{r}) \right|^2, \qquad (1)$$

where N_c is the coordination number, and vector $\mathbf{r}$ refers to the atom and its nearest neighbors in an (defective) fcc solid or its melt under consideration. The first minimum distance in the radial distribution function (RDF) is taken as the nearest-neighbor distance. ψ is essentially a local static structure factor. Averaging ψ among an atom and its N_c nearest neighbors yields an averaged local order parameter of this atom,[22,23] $\bar{\psi}$, which is used for characterizing local disordering. The global order parameter (Ψ) is the average of ψ over all the atoms in the system. Similar simulation and analysis details were presented elsewhere.[10,23]

A solid can be distinguished from its melt with diffusion coefficient (D); D for a solid can be 1–3 orders of magnitude lower than its liquid counterpart. D can be calculated from the mean squared displacement (MSD) with the Einstein expression,[24] MSD $= 6Dt$, or from the slope of MSD(t), where t denotes time. MSD is defined as

$$\text{MSD} = \langle |\mathbf{r}(t) - \mathbf{r}(0)|^2 \rangle. \qquad (2)$$

Here $\mathbf{r}$ is atomic position.

III. RESULTS AND DISCUSSION

Our simulations regarding GB melting on two system sizes yield similar results; however, the simulations on the smaller system offer more details, and are thus adopted in the following discussions. During incremental heating, bulk melting is characterized by discontinuous changes in such physical properties as enthalpy, density and global ordering. Shown in Fig. 2 and Fig. 3 inset are the temperature evolutions of the atomic volume and the global order parameter obtained at the end of the run for each temperature. (The variation of local order parameters with T is shown in Fig. 1.) The average atomic volume (V) increases and Ψ decreases steadily with T up to 1480 K; however, V increases rapidly by 2.3% at 1500 K and Ψ decreases from 0.47 at 1480 K to 0.19 at 1500 K. Complete melting occurs at 1520 K with $\Psi \approx 0.115$ (Fig. 3); we thus define an atom to be liquid if $\bar{\psi} \leq 0.115$. Note that this condition is necessary rather than sufficient for describing a liquid state since $\bar{\psi} = 0.115$ only represents an average of all the atoms within a liquid. A liquid consists of atoms with $\bar{\psi} > 0.115$ and $\bar{\psi} \leq 0.115$. The thermodynamic equilibrium melting temperature for Cu as predicted by the EAM potential is $T_m \approx 1325 \pm 20$ K.[23] At current heating rate (20 K per 50 ps), the maximum superheating temperature (T_+) is 1500 K where bulk melting of the system begins. For comparison, T_+ is about 1620 K for an initially perfect solid (Fig. 2).

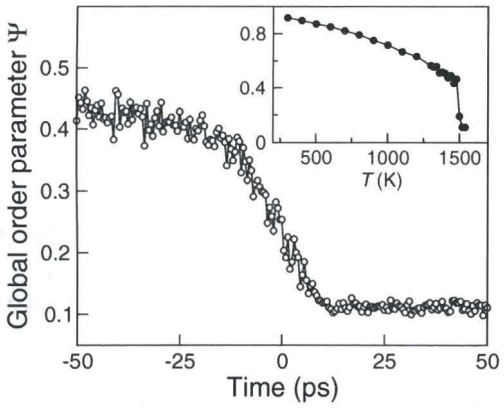

FIG. 3: Temporal evolution of the global order parameter of the Cu bicrystal, $\Psi(t)$, at 1500 K (0–50 ps) and 1520 K (50–100 ps). Inset: Ψ versus temperature during incremental heating.

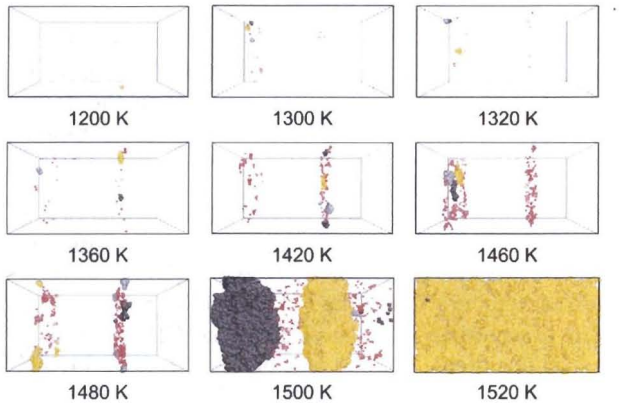

FIG. 4: Configurations of strict liquid atoms during incremental heating of the Cu bicrystal after 50 ps thermalization at respective temperatures. Color coding refers to the liquid cluster size. Atoms in the first, second and third largest clusters are colored yellow, black and gray, respectively; the rest are colored red.

The high energy GBs reduce the amount of superheating from $0.22T_m$ to $0.13T_m$. Nonetheless, the bicrystal is still superheated noticeably as far as GB bulk melting is concerned. (See below for more discussion on bulk melting of GB.)

The temperature evolutions of the local order parameters (Fig. 1) and of the liquid atoms (Fig. 4) indicate that heterogeneous nucleation and growth at the GBs dominate melting. Disordering is pronounced along GBs and its spatial variations can be regarded as one dimensional along the GB normal. To characterize the order parameter across the planar GBs, we divide the simulation cell along the interface normal (the x direction) into small bins and Ψ is calculated for each bin, yielding a profile $\Psi(x)$. Shown in Fig. 5(a) is such an example obtained at 1500 K and $t = 47.5$ ps. The profile of the order

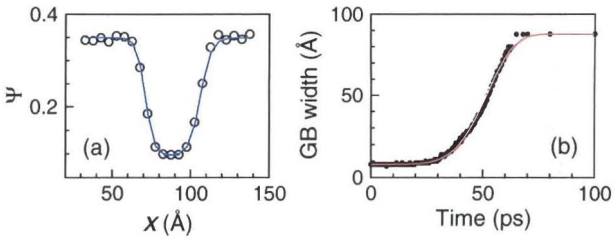

FIG. 5: (a) The order parameter profile along x-axis of the heated bicrystal at 1500 K and 47.5 ps. The solid curve is the fitting with Eq. (3). (b) GB width versus time at 1500 K. The fitting (solid curve) refers to Eq. (4).

parameter can be described with a sigmoid function

$$\Psi(x) = \Psi_1 + \frac{\Psi_2 - \Psi_1}{2}\left[1 - \tanh\left(\frac{x - x_0}{2w}\right)\right]. \qquad (3)$$

Here x_0 is the center of a solid-liquid interface, and w represents a characteristic length sale of the interface. The subscripts 1 and 2 refer to the high and low plateau values, respectively. We take the thickness of a GB, d, as the full width at half maximum (FWHM) of the order parameter profile.

Given the GB thickness defined above, we examine the growth kinetics of melt originated at GBs. The temporal evolution of the GB thickness at 1500 K during a 100 ps run is shown in Fig. 5(b), and can be described with

$$d(t) = d_1 + (d_2 - d_1)\left[1 - \exp(-kt^\eta)\right], \qquad (4)$$

where d_1, d_2, k and η are parameters. Here subscripts 1 and 2 refer to the initial thickness and that at complete melting, respectively, for a particular isobaric and isothermal run. η is characteristic of the growth kinetics of the GB region, and is about 5.6 for growth of melt at 1500 K. (This equation is similar in formality to the Johnson-Mehl-Avrami law.[25,26]) The melting kinetics are sensitive to temperature. A slight decrease in temperature slows down the kinetics. For example, bulk melting and growth occur at about 1.2 ns and $\eta \sim 4$ at 1480 K. The corresponding values are about 30 ps and 5.6, respectively, at 1500 K. During melting, the solid-liquid interface moves and its velocity is normally considered to be a constant.[12] However, Fig. 5(b) shows the interface velocity increases as bulk melting progresses and reaches roughly a constant value before complete melting. This velocity (for a single interface) is about 150 $\mathrm{m\,s^{-1}}$ and 120 $\mathrm{m\,s^{-1}}$ at 1500 K and 1480 K, respectively.

It is highly desirable to investigate in detail the characteristics of GB during heating in order to gain insight into GB melting. The evolution of the GB width during stepped heating is shown in Fig. 6(a); d increases gradually from 300 K to 1480 K, and then abruptly from 1480 K to 1500 K. The GB width increases from about 5 Å at 300 K to 6.5 Å at 1300 K and then to 9.5 Å at 1480 K. The abrupt increase in GB width at 1500 K is

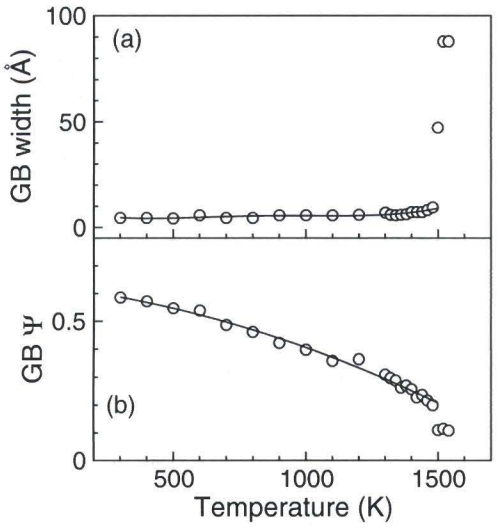

FIG. 6: Temperature evolution of GB width (a) and of the GB order parameter for a fixed width of 5 Å (b).

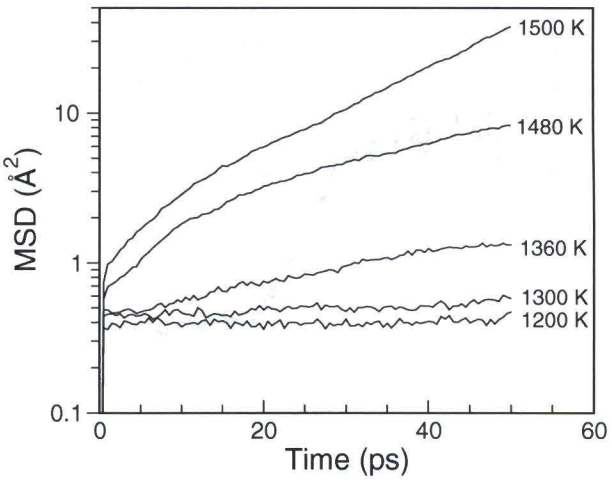

FIG. 7: Time evolution of MSD of the Cu bicrystal during incremental heating, within the central 5 Å of the GB.

consistent with the density and global order parameter for the whole system (Figs. 2 and 3). A relevant question is whether GB melting occurs in the range of 300 K–1480 K. We thus characterize the structure features of the central 5 Å region within the GBs in terms of Ψ defined for this region at different temperatures; $\Psi_{GB}(T)$ shows a similar trend to the GB width (Fig. 6). Ψ_{GB} decreases continuously from about 0.6 at 300 K to 0.2 at 1480 K then drops to about 0.11 at 1500 K ($\Psi = 0.115$ for liquid). Thus, the center region of GB as a whole is not melted for $T < 1500$ K. The complete melting of the GB region as a whole occurs at 1500 K and this is called bulk melting of GB. GB bulk melting is the first order in nature, i.e., discontinuous changes occur in the temperature evolutions of certain physical properties [e.g., Fig. 6(b)].

We examine further the GB melting with MSD and diffusion coefficients in the central 5 Å GB region. The MSD evolutions at some selected temperatures are shown in Fig. 7; we also calculate the MSD of the initially perfect solid as well as liquid at 1300 K–1600 K (not shown) for comparion. At a given temperature, MSD increases rapidly at the beginning (ballistic regime), and then it either reaches a plateau or grows with a slope. This slope is characteristic of diffusion. In both cases (perfect and defective solids), the slope increases steadily with temperature until 1500 K and 1620 K, respectively, where the slope increase becomes drastic. (Note the logarithm scale for MSD in Fig. 7.)

If the GB melts as a whole, D in the central 5 Å region should be close to that of a liquid at the same temperature. For the Cu liquid, $D(T)$ can be described with an Arrhenius relation, increasing from about 3×10^{-9} m^2 s^{-1} at 1300 K to 5×10^{-9} m^2 s^{-1} at 1600 K. For GB, the slope increase in MSD(t) becomes noticeable around T_m (1325±20 K), where D is only about 7×10^{-12} m^2 s^{-1}. D increases to 3×10^{-10} m^2 s^{-1} at 1480 K. Therefore, D is about 1–3 orders of magnitude lower than the liquid counterparts at 1320 K–1480 K. However, D becomes about 4×10^{-9} m^2 s^{-1} at 1500 K, similar to 4.4×10^{-9} m^2 s^{-1} for the liquid at the same temperature. Thus, the GB as a whole only melts at 1500 K. The melting of *GB as a whole* is *not* a continuous process since the discontinuous changes in, e.g., V, Ψ, D and enthalpy occur in a narrow temperature range (1480 K–1500 K).

The above analyses suggest that, the GB region as a whole is not premelted and is superheated up to 1480 K before discontinuous bulk melting. Below T_m, very few strict liquid atoms are observed (Fig. 4); thus, localized premelting is negligible and the disordering in the GB region is dominantly *solid-state disordering* rather than melting. Local melting in the form of scattered liquid nuclei (Fig. 4) and solid state disordering coexist at $T \geq T_m$. This transient coexistence of solid and liquid phases is due to kinetics, and gives rise to the "seemingly continuous" melting. We discuss below the continuous local melting in the GB region which is bulk superheated.

Fig. 4 shows that (strict) liquid atoms only occur near the GBs, i.e., the homogeneous nucleation is essentially totally suppressed at $T < 1500$ K. The liquid atoms forms isolated nuclei (islands) with fluctuating sizes and locations. This suggests local melting rather than bulk melting of GB. The temperature evolutions of liquid nuclei are characterized in Fig. 8 in terms of cluster size distribution via cluster analysis. Two atoms belong to the same cluster or nucleus if they are within the nearest-neighbor distance (obtained from RDF) of each other. The cluster size is the number of atoms contained in this cluster. The liquid clusters nucleated around the GBs connect into a single one at 1500 K (GB bulk melting) as demonstrated by the rapid growth of the largest cluster and the reduction in the number of nuclei centered near

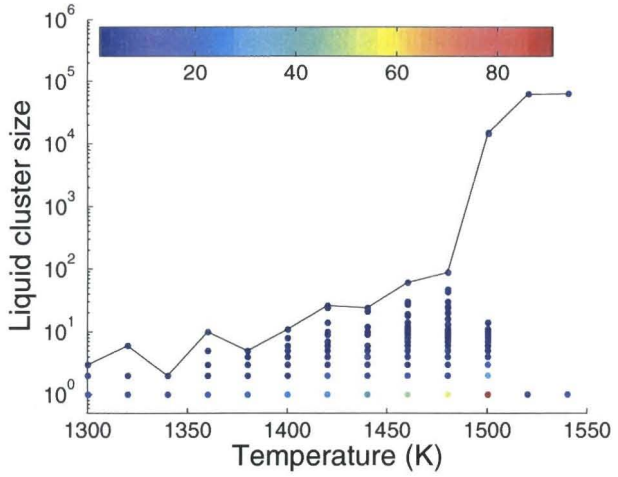

FIG. 8: Size distribution of liquid cluster at different temperatures for the heated Cu bicrytsal. The color coding and the color scale bar denote multiplicity (or frequency) of the cluster with a given size. The solid curve refers to the largest cluster.

the GB. (The nuclei with a cluster size below 10 at 1500 K are off the GB and largely due to homogeneous nucleation.) Thus, continuous local melting precedes discontinuous bulk melting of the GB. This local melting is in contrast to the explicit or tacit assumption in literature that grain boundary melting begins with a thin uniform liquid layer occupying the whole GB region. The local melting at GB is difficult to observe experimentally due to the limited spatial and temporal resolutions in real experiments.

Lindemann parameters[27–29] are not appropriate for partial melting and liquid since the mean squared displacement increases with time rather than reaches a well defined plateau (Fig. 7). The gradual slope rise of the liquid-like MSD(t) indicates partial melting (local melting), but complete (bulk) melting is well defined by comparing diffusion efficient to the liquid counterpart. Thus it is necessary to differentiate local and bulk melting as regards GB melting. Since superheating depends on heating rate,[30] the amount of superheating should be reduced at heating rates lower than in MD simulations. The issue of whether or not the GB premelts at low heating rates remains open, although in previous low heating rate experiments the amount of premelting is small or negligible.[11] In this regard, we expect our results here may also apply to low heating rates.

IV. CONCLUSION

At conventional MD simulation time scales, continuous solid state disordering of the GBs occurs at temperatures below T_m, and no noticeable premelting is observed within simulation uncertyainties. Local melting initiates near T_m in the form of scattered liquid nuclei and progresses continuously. Since local melting is kinetically limited, the GB region as a whole is superheated by about $0.13T_m$ before its bulk melting occurs discontinuously.

Acknowledgments

L.B.H. and Q.A. acknowledge the support from NSF of China Grants No. 40574043 and 40425005. L.Z. is grateful for W. Yang's support. S.N.L. is partially supported by an LDRD-DR program (T.C. Germann) at LANL. LANL is under the auspices of U.S. Department of Energy under contract No. DE-AC52-06NA25396. We have benefited from discussions with S. Zhao.

* Currently at Materials and Process Simulation Center, California Institute of Technology.
† Electronic address: sluo@lanl.gov

[1] J. W. Christian, *The Theory of Transformation in Metals and Alloys* (Pergaman, New York, 1965).
[2] H. Kleinert, *Gauge Fields in Condensed Matter* (World Scientific, Singapore, 1989).
[3] J. G. Dash, *Films of Solid Surface* (Academic Press, London, 1975).
[4] J. D. Honeycutt and H. C. Andersen, J. Phys. Chem. **91**, 4950 (1987).
[5] L. Gomez, A. Dobry, C. Geuting, H. T. Diep, and L. Burakovsky, Phys. Rev. Lett. **90**, 095701 (2003).
[6] J. Solca, A. J. Dyson, G. Steinebrunner, B. Kirchner, and H. Huber, Chem. Phys. **224**, 253 (1997).
[7] P. M. Agrawal, B. M. Rice, and D. L. Thompson, J. Chem. Phys. **119**, 9617 (2003).
[8] S. N. Luo, L. Q. Zheng, and O. Tschauner, J. Phys.: Condens. Matter **18**, 659 (2006).
[9] S. Link, Z. L. Wang, and M. A. El-Sayed, J. Phys. Chem. B **104**, 7867 (2000).
[10] L. B. Han, Q. An, R. S. Fu, L. Q. Zheng, and S. N. Luo, J. Chem. Phys., in press (2008).
[11] B. Chalmers, J. W. Christian, and T. B. Massalski, Prog. Mat. Sci. **16**, 13 (1972).
[12] J. F. Lutsko, D. Wolf, S. R. Phillpot, and S. Yip, Phys. Rev. B **40**, 2841 (1989).
[13] S. F. Xiao and W. Y. Hu, J. Chem. Phys. **125**, 014503 (2006).
[14] A. M. Alsayed, M. F. Islam, J. Zhang, P. J. Collings, and A. G. Yodh, Science **309**, 1207 (2005).
[15] W. Fan and X. G. Gong, Phys. Rev. B **72**, 064121 (2005).
[16] S. J. Zhao, S. Q. Wang, T. G. Zhang, and H. Q. Ye, J. Phys.: Condes. Matter **34**, L549 (2000).
[17] G. Ciccotti, M. Guillope, and V. Pontikis, Phys. Rev. B **27**, 5576 (1983).
[18] J. D. Rittner and D. N. Seidman, Phys. Rev. B **54**, 6999 (1996).

[19] Y. Mishin, M. J. Mehl, D. A. Papaconstantopoulos, A. F. Voter, and J. D. Kress, Phys. Rev. B **63**, 224106 (2001).
[20] W. G. Hoover, Phys. Rev. A **31**, 1695 (1985).
[21] J. Stadler, R. Mikulla, and H.-R. Trebin, Int. J. Mod. Phys. C **8**, 1131 (1997).
[22] J. R. Morris and X. Song, J. Chem. Phys. **116**, 9352 (2002).
[23] L. Q. Zheng, Q. An, Y. Xie, Z. H. Sun, and S. N. Luo, J. Chem. Phys. **127**, 164503 (2007).
[24] D. C. Rapaport, *The Art of Molecualr Dynamics Simulation* (Cambridge University Press, 1995).
[25] M. Avrami, J. Chem. Phys. **8**, 212 (1940).
[26] W. A. Johnson and R. F. Mehl, Am. Inst. Min. Met. Engrs. – Trans. **135**, 416 (1939).
[27] F. A. Lindemann, Phys. Z. **11**, 609 (1910).
[28] J. J. Gilvarry, Phys. Rev. **102**, 308 (1956).
[29] S. N. Luo, A. Strachan, and D. C. Swift, J. Chem. Phys. **122**, 194709 (2005).
[30] S. N. Luo, T. J. Ahrens, T. Çağın, A. Strachan, W. A. Goddard III, and D. C. Swift, Phys. Rev. B **68**, 134206 (2003).